ISAC-STAP: Space-time Adaptive Processing for ISAC Systems

Nakyung Lee, Hyunwoo Park, Hanvit Kim, Kyung-Young Jung, Sunwoo Kim
Department of Electronic Engineering, Hanyang University, Seoul, South Korea
nagyeong2379, stark95, dante0813, kyjung3, remero @hanyang.ac.kr

2024 IEEE Globecom Workshops (GC Wkshps) | 979-8-3315-0567-7/24/$31.00 ©2024 IEEE | DOI: 10.1109/GCWkshp64532.2024.11101537

***Abstract*—This paper proposes space-time adaptive processing (STAP) for integrated sensing and communication (ISAC) systems. In the scenarios where a moving ISAC transceiver is sensing targets, clutter with nonzero Doppler shift complicates the task of distinguishing targets from clutter. The proposed algorithm improves target sensing performance by suppressing clutter with nonzero Doppler shift via leveraging the STAP algorithm. Through pre-processing, the proposed algorithm converts the echo of the transmitted communication signal into a radar-like data cube. Then, the proposed algorithm utilizes the range cells near the target to suppress clutter in the target's range cell and estimate the target's parameters. Simulation results demonstrate the superiority of the proposed algorithm in clutter suppression and target sensing in mobile ISAC systems, providing a convincing case for its adoption over existing ISAC target sensing algorithms.**

***Index Terms*—ISAC, moving target sensing, STAP, clutter suppression, moving transceiver**

I. Introduction

Integrated sensing and communications (ISAC) has been considered a key technology for next-generation communications since it can provide high-quality wireless connectivity and robust sensing capabilities, which the B5G/6G demands [1]. The primary function of ISAC is to utilize communication signals for dual purposes: environmental sensing and high-quality communication [1]–[3]. This dual functionality allows ISAC to efficiently share spectrum resources while minimizing equipment size and energy consumption [4]. Due to these advantages, ISAC has gained significant attention, and both the International Telecommunication Union and Hexa-X-II regard it as a key enabler for future wireless communication systems [5], [6].

One of the notable technologies for ISAC is echo signal processing, focusing on estimating the target's parameters such as location, range, and velocity [7]–[9]. Most of the echo signal processing studies for ISAC have mainly considered the ideal scenario where the ISAC transceiver only receives reflected signal from the target of interest [10]–[12]. However, in practical applications, the ISAC transceiver receives the reflected signals not only from targets but also from clutter that interferes with target sensing. This clutter from surrounding objects such as ground, buildings, and trees causes interference, degrading the target sensing performance.

This work was supported by the National Research Foundation of Korea(NRF) grant funded by the Korea government(MSIT) (No. NRF-2023R1A2C3002890).

Although clutter reflection critically degrades sensing performance in ISAC, only a few studies have considered clutter environments. In [13], an optimization framework is proposed to maximize the sensing beamforming gain for targets, subject to the power constraints of each clutter. In [14], a space-time adaptive processing (STAP) algorithm is adopted for clutter suppression in ISAC systems. However, the clutter suppression algorithms proposed in [13] and [14] are unsuitable for practical scenarios because these algorithms require prior knowledge of the clutter, which is commonly unavailable. In [15], a Doppler-domain clutter suppression algorithm was proposed by assuming that the Doppler frequency of static clutter is zero. Similarly, in [16], a search space-based clutter suppression algorithm was proposed, relying on the same assumption. However, the algorithms in [15] and [16] are not applicable to the mobile ISAC systems, where the clutter has a non-negligible Doppler shift due to the mobility of the ISAC transceiver.

To enhance target sensing performance in mobile ISAC applications, such as simultaneous localization and mapping [17] and vehicle-to-everything (V2X) communication [18], this paper proposes an ISAC-STAP algorithm. The proposed algorithm first pre-processes the received echo signal by converting the subcarrier & beam domain into the range & antenna domain. After pre-processing, the clutter in the target's range is suppressed using the neighboring range cells, and the target's channel parameters are estimated in the mobile ISAC systems. Here, the performance of clutter suppression is reinforced by leveraging spatio-temporal adaptive filtering, which enables more accurate target sensing compared to existing target sensing algorithms in ISAC systems.

Notations: For a matrix $\mathbf{A}$, its transpose, Hermitian transpose, and inverse are respectively denoted as $\mathbf{A}^{\mathsf{T}}$, $\mathbf{A}^{\mathsf{H}}$, and $\mathbf{A}^{-1}$. The symbol $\jmath$ represents the imaginary unit of complex numbers, ($\jmath = \sqrt{-1}$). $\mathbf{I}_N$ denotes a $N \times N$ identity matrix. $\mathbf{A}[i,:]$ and $\mathbf{A}[:,j]$ denote the i-th row and the j-th column of the matrix $\mathbf{A}$. Similarly, $\mathcal{A}[i,:,:]$ and $\mathcal{A}[:,:,j]$ represent the i-th slice along the first dimension and the j-th slice along the third dimension of a 3D tensor $\mathcal{A}$, repectively. $\mathbb{E}[\cdot]$ denotes the statistical expectation operator and $\otimes$ denotes the Kronecker product.

II. System Model

We consider an ISAC system in which a moving ISAC transceiver is monostatically sensing targets in a cluttered

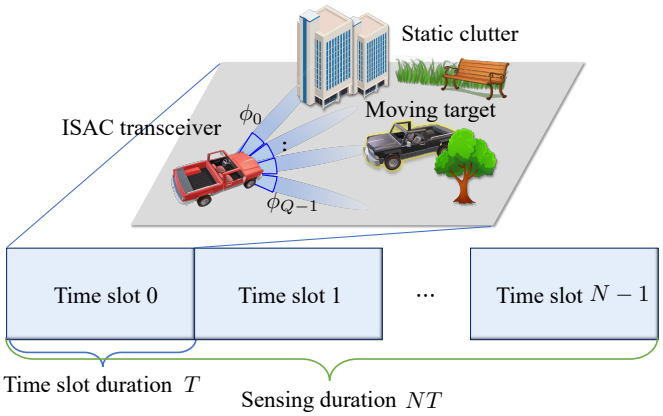

Fig. 1. The considered ISAC framework. The moving ISAC transceiver transmits sensing beams for dynamic target sensing in mobile ISAC systems with static clutter and moving target.

environment. A uniform linear array (ULA) antenna consisting of M elements is attached vertically to the direction of the ISAC transceiver's moving direction. The spacing between the antenna elements is set as $d = \lambda\ 2$, where λ is the carrier wavelength.

During an ISAC sensing duration, the ISAC transceiver transmits and receives the echo signal reflected by the targets and clutter for N time slots, where the time slot duration is T as shown in Fig. 1. Here, we assume that the channel is stationary within a time slot [19]. For ISAC sensing and communication, the ISAC transceiver transmits Q codebook beams in a time slot, where the ISAC signal of each beam is modulated as OFDM with L subcarriers. The frequency of the l-th subcarrier is $f_l = f_0 + l\Delta f$ for $l = 0\ 1\ \cdots\ L-1$, where f_0 is the carrier frequency and Δf is the subcarrier spacing.

The transmitted ISAC signal of ULA is the multiplication of beamforming vector $\mathbf{w}_q$ and OFDM data symbol $s_{n\,q\,l}$ represented as [15]

$$\mathbf{x}_{n\,q\,l} = \mathbf{w}_q s_{n\,q\,l} \quad \mathbb{C}^{M\times 1} \tag{1}$$

where n, q and l are the index of time slot, beam and subcarrier respectively. The codebook beamforming vector $\mathbf{w}_q$ is represented as

$$\mathbf{w}_q = \sqrt{\frac{P_{\mathrm{T}}}{M}}\mathbf{a}(\phi_q) \quad \mathbb{C}^{M\times 1} \tag{2}$$

where P_{T} is the transmission power of ISAC transceiver and $\mathbf{a}(\phi_q)$ is the steering vector for the angle ϕ_q. The steering vector for a general angle θ is formulated as

$$\mathbf{a}(\theta) = \left[1\ \ e^{\,\pi\sin\theta}\ \ \cdots\ \ e^{\,\pi(M-1)\sin\theta}\right]^{\mathsf{T}} \quad \mathbb{C}^{M\times 1} \tag{3}$$

The transmitted signal is reflected by the targets and clutter, and is received with the same beam used for the transmission. The received echo signal corressponding to the transmitted signal $\mathbf{x}_{n\,q\,l}$ is expressed as [15]

$$y_{n\,q\,l} = \mathbf{w}_q^{\mathsf{H}}\mathbf{H}_{n\,l}\mathbf{x}_{n\,q\,l} + z_{n\,q\,l} \tag{4}$$

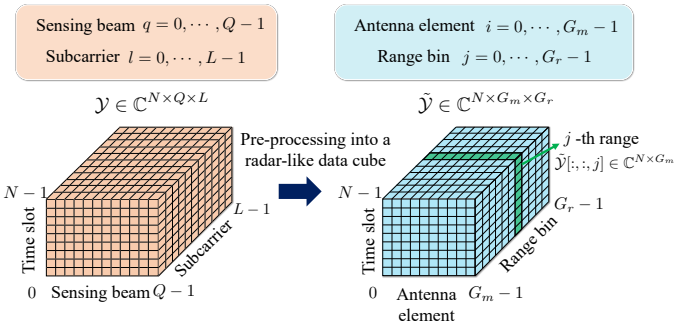

Fig. 2. The pre-processing of the proposed ISAC-STAP.

where $z_{n\,q\,l}$ is the additive white Gaussian noise with the noise power $\sigma^2_{n\,q\,l}$. The round-trip channel $\mathbf{H}_{n\,l}$ for K targets and P static clutter is represented as [15]

$$\mathbf{H}_{n\,l} = \sum_{k=1}^{K}\mathbf{H}_{k\,n\,l} + \sum_{p=1}^{P}\mathbf{H}'_{p\,n\,l} \quad \mathbb{C}^{M\times M} \tag{5}$$

where $\mathbf{H}_{k\,n\,l}$ is the round-trip channel of k-th target and $\mathbf{H}'_{p\,n\,l}$ is the round-trip channel of p-th clutter. Here, $\mathbf{H}_{k\,n\,l}$ and $\mathbf{H}'_{p\,n\,l}$ are represented as

$$\mathbf{H}_{k\,n\,l} = \alpha_k e^{\,2\pi f_0 f_{D\,k} nT} e^{-\,2\pi f_l \frac{2r_k}{c}}\mathbf{a}\left(\theta_k\right)\mathbf{a}^{\mathsf{H}}\left(\theta_k\right) \tag{6}$$

$$\mathbf{H}'_{p\,n\,l} = \beta_p e^{\,2\pi f_0 f'_{D\,p} nT} e^{-\,2\pi f_l \frac{2r'_p}{c}}\mathbf{a}\left(\theta'_p\right)\mathbf{a}^{\mathsf{H}}\left(\theta'_p\right) \tag{7}$$

where $(\alpha_k\ r_k\ \theta_k)$ and $(\beta_p\ r'_p\ \theta'_p)$ are the channel fading factor, distance and angle pair of the k-th target and the p-th clutter respectively and c is the speed of light. $f_{D\,k} = 2\ (\mathbf{v}_R - \mathbf{v}_k)\ \boldsymbol{k}(\theta_k)\ \ c$ and $f'_{D\,p} = 2\ \mathbf{v}_R\ \boldsymbol{k}(\theta'_i)\ \ c$ are the relative Doppler shift of the k-th target and the p-th clutter, where $\mathbf{v}_R$ is the velocity of ISAC transceiver and $\mathbf{v}_k$ is the velocity of k-th target. $\boldsymbol{k}(\theta)$ is a unit vector pointing towards θ direction. Note that, due to the transceiver's mobility, the clutter's relative Doppler shift is also nonzero, making it challenging to distinguish the target. Eventually, the echo tensor $\mathcal{Y}\ \ \mathbb{C}^{N\times Q\times L}$ is measured by stacking $y_{n\,q\,l}$, whose $(n\ q\ l)$-th element is $\mathcal{Y}[n\ q\ l] = y_{n\,q\,l}$.

III. ISAC-STAP for Clutter Suppression and Target Sensing

In this section, we propose the ISAC-STAP algorithm, which suppresses the clutter with nonzero Doppler shift and estimates the target parameters. The proposed algorithm converts the echo tensor into a radar-like data cube through pre-processing. Thereafter, the proposed algorithm detects the targets by suppressing the clutter via estimating the clutter covariance matrix by utilizing range cells near the target range.

A. Pre-processing of the Echo Tensor

The basic idea of STAP is to design a filter that removes clutter signals by finding out clutter information from the measurement. Since prior STAP algorithms utilize pulsed radar, the measurement has the range domain and the clutter in the target range is eliminated by using clutter information in

the range where the target is not present. However, the ISAC transceiver system under consideration does not operate within a specific range domain, and the target's echo signal impacts all the elements of the measurement. Therefore, the proposed algorithm pre-processes the measurement by converting echo tensor $\mathcal{Y}$ into a radar-like data cube.

The key idea of the pre-processing is to convert the domain of $\mathcal{Y}$ same as the domain of radar data cube, which are array antenna elements, time slots and range bins. Interestingly, the domains of OFDM subcarrier and range, as well as beam and antenna array elements, are all discrete Fourier transform (DFT) related. By implementing two-dimensional DFT (2D-DFT), the $\mathcal{Y}$ is pre-processed to a radar-like data cube $\mathcal{Y} \quad \mathbb{C}^{N\times G_m\times G_r}$ as in Fig. 2, and the elements are calculated as

$$\mathcal{Y}[n\ i\ j] = \mathbf{s}_{A\,i}^{\mathsf{T}}\mathcal{Y}[n\ :\ :]\mathbf{s}_{R\,j} \tag{8}$$

where $\mathbf{s}_{A\,i} \quad \mathbb{C}^{Q\times 1}$ is the DFT vector to vurtual antenna elements, and $\mathbf{s}_{R\,j} \quad \mathbb{C}^{L\times 1}$ is the DFT vector to range bins respectively expressed as

$$\mathbf{s}_{A\,i} = \left[1\ e^{-\,\pi\sin\phi_i}\ \cdots\ e^{-\,\pi(Q-1)\sin\phi_i}\right]^{\mathsf{T}} \tag{9}$$

$$\mathbf{s}_{R\,j} = \left[1\ e^{-\,2\pi\frac{2\tilde{r}_j}{c}\Delta f}\ \cdots\ e^{-\,2\pi\frac{2\tilde{r}_j}{c}(L-1)\Delta f}\right]^{\mathsf{T}} \tag{10}$$

where ϕ_i for $i = 1\ 2\ \cdots\ G_m$ is the angle bins and r_j for $j = 1\ 2\ \cdots\ G_r$ is the range bins. G_m and G_r are the number of virtual antenna elements (same with number of angle bins) and range bins respectively.

B. Clutter Suppression and Target Sensing

Since the distribution of clutter changes over time due to the mobility of ISAC transceiver, it is not possible to obtain clutter information in advance. Therefore, the proposed approach employs the principle of sample matrix inversion (SMI) STAP [20], which does not require any prior information about clutter or targets.

The principle of SMI STAP is to construct a spatio-temporal adaptive filter that maximizes the signal-to-interference-plus-noise ratio (SINR) for the cell under test. By applying the filter across the entire range, the ranges with values higher than the threshold are determined as the target range. For the decision of the presence of a target-of-interest in j-th range, the scalar output z_j, is calculated as [20]

$$z_j = \mathbf{w}_j^{\mathsf{H}}\boldsymbol{\eta}_j \tag{11}$$

where $\mathbf{w}_j \quad \mathbb{C}^{NG_m\times 1}$ is the weight vector that maximizes SINR in j-th range and $\boldsymbol{\eta}_j = \mathrm{vec}\left(\mathcal{Y}[:\ :\ j]\right) \quad \mathbb{C}^{NG_m\times 1}$ is the space-time snapshot of j-th range. The optimal weight vector $\mathbf{w}_j^*$ for j-th range follows [20]

$$\mathbf{w}_j^* = \mathbf{R}_j^{-1}\mathbf{v}(\nu\ \theta) \tag{12}$$

where $\mathbf{R}_j$ is the interference covariance matrix which is unknown in practice. $\mathbf{v}(\nu\ \theta)$ is the space-time steering vector expressed as

$$\mathbf{v}(\nu\ \phi) = \mathbf{a}(\nu)\otimes\mathbf{b}(\phi) \tag{13}$$

TABLE I. Simulation parameters

Parameter	Description	Value
f_0	Carrier frequency	24.125 GHz
Δf	Subcarrier spacing	120 kHz
M	Number of ULA element	32
N	Number of OFDM symbols	64
Q	Number of sensing beam	121
L	Number of OFDM subcarriers	128
P	Number of clutters	5000
G_m	Number of angle bins	121
G_r	Number of range bins	128

where $\mathbf{a}(v)$ is the temporal steering vector for the radial velocity ν

$$\mathbf{a}(\nu) = \left[1\ e^{-\,2\pi\nu\frac{T}{\lambda}} \quad e^{-\,2\pi(N-1)\nu\frac{T}{\lambda}}\right]^{\mathsf{T}} \quad \mathbb{C}^{N\times 1} \tag{14}$$

and $\mathbf{b}(\phi)$ is spatial steering vector for the angle ϕ

$$\mathbf{b}(\phi) = \left[1\ e^{\,\pi\sin\phi} \quad e^{\,\pi(G_m-1)\sin\phi}\right]^{\mathsf{T}} \quad \mathbb{C}^{G_m\times 1} \tag{15}$$

Since the interference covariance matrix $\mathbf{R}_j$ for the target range is unknown, it is estimated by the training range cells which are near to the target range cell. The interference covariance matrix is estimated as [21]

$$\mathbf{R}_j = \frac{1}{R}\sum_{r=1}^{R}\boldsymbol{\eta}_r\boldsymbol{\eta}_r^{\mathsf{H}} \tag{16}$$

where R is the number of training range cells, and $\boldsymbol{\eta}_r\ _{r=1}^{R}$ are the training range cells. While suppressing clutter, the actual target signal suffers from unintentional suppression along with the clutter, which refers to target self-whitening. To prevent target self-whitening, the STAP processor excludes the several adjacent cells, referred to as guard cells, from the training range cells. Finally, with the estimated interference covariance matrix, the weight vector $\mathbf{w}_j$ for j-th range is constructed as

$$\mathbf{w}_j = \mathbf{R}_j^{-1}\mathbf{v}(\nu\ \theta) \tag{17}$$

IV. Simulation Results and Discussions

In the simulation, we first verify the clutter suppression and the target range estimation availability of the proposed algorithm in a single episode. Then, we analyze the root mean square error (RMSE) performance of the target parameter estimation over the velocity of ISAC transceiver. To verify the effectiveness in the mobile ISAC systems, the proposed algorithm is compared with H. Luo et al. [15]. The parameter settings that are used in every simulation are listed in Table I.

First, we consider an episode where ISAC transceiver is sensing two targets while moving with a velocity of $\mathbf{v}_R = [50\ 0]$ m/s. The targets parameters are set as

$$\begin{aligned}\theta_1\ r_1\ \mathbf{v}_1 &= \pi\ 4\ 98\,995\ \text{m}\ [10\ 10]^{\mathsf{T}}\ \text{m/s}\\ \theta_2\ r_2\ \mathbf{v}_2 &= -\pi\ 4\ 70\,711\ \text{m}\ [-30\ -30]^{\mathsf{T}}\ \text{m/s}\end{aligned} \tag{18}$$

Normalized power spectrum at the target 1's range is shown in Fig. 3, where Fig. 3a, Fig. 3b and Fig. 3c are the spectrum before clutter suppression, after processing the algorithm of

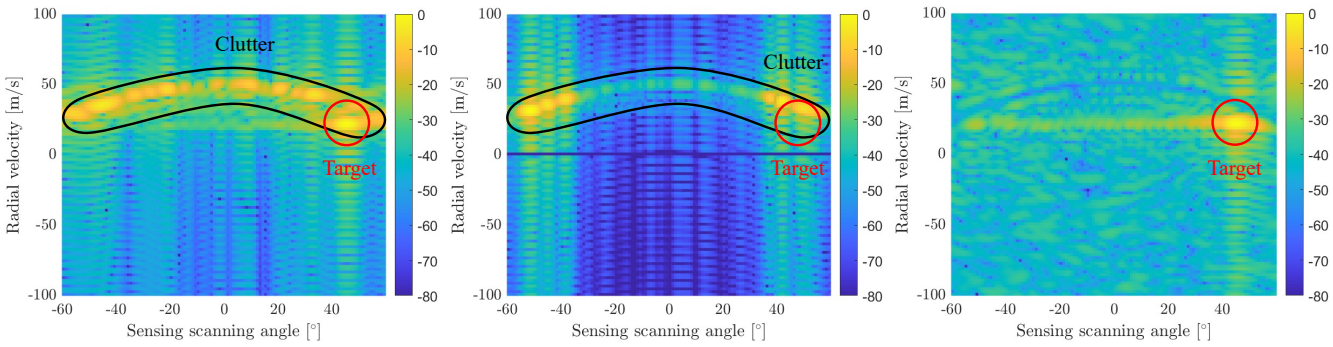

(a) Before clutter suppression (b) H. Luo et al. [15] (c) Proposed ISAC-STAP

Fig. 3. Normalized power spectrum [dB] at the range cell of target 1 (64-th range cell)

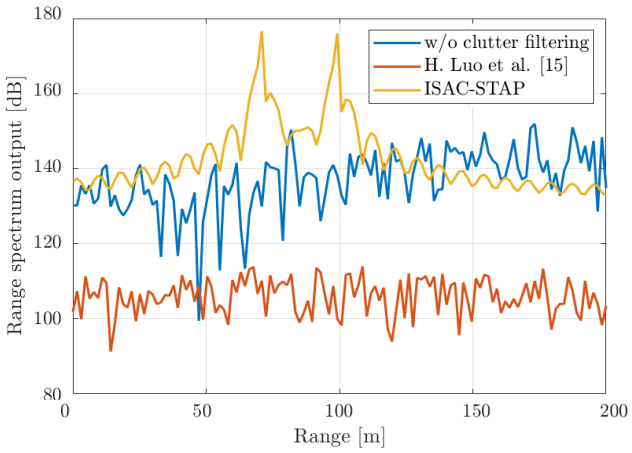

Fig. 4. Target range scanning results.

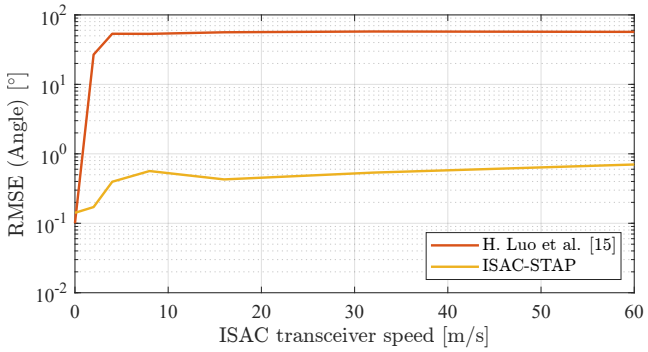

(a) RMSE of angle estimation

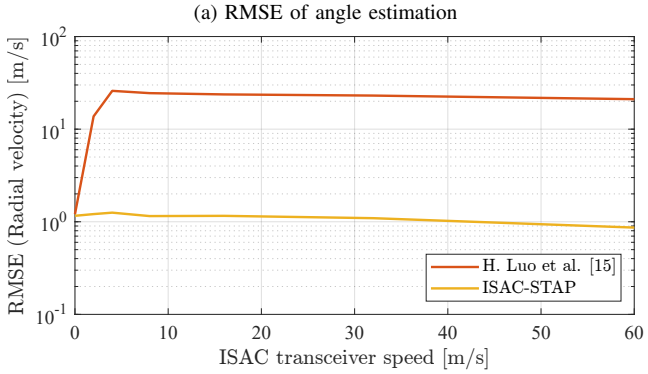

(b) RMSE of radial velocity estimation

Fig. 5. RMSE of target's parameter estimation along the ISAC transceiver speed.

[15], and after processing ISAC-STAP respectively. Since the ISAC transceiver has the mobility, we can observe from the power distribution in Fig.3a that the clutter has a non-zero radial velocity with varying values across angles. The power spectrums after clutter suppression show the different strategies of [15] and ISAC-STAP. Since H. Luo et al. [15] suppresses the signal with zero velocity, the clutter spectrum remains, and the target is suppressed as shown in Fig. 3b. Therefore, there is a high probability that the clutter might be mistaken as the target. On the other hand, ISAC-STAP accurately removes clutter by using the surrounding ranges information, leaving only the target signal as shown in Fig. 3c. This improvement demonstrates the robustness of the proposed algorithm in suppressing the clutter caused by the mobility of the ISAC transceiver.

The target range scanning results are shown in Fig. 4. The range spectrum output is calculated by dB scaling the scalar output z_j in (11) to decide the range of a target-of-interest. The echo signal without clutter suppression shows significant fluctuations along the ranges, indicating high levels of interference within the signal. Even though H. Luo et al. [15] reduces the overall spectrum by suppressing the zero-velocity components, there is no improvement in SINR, so the target range estimation performance remains unchanged. In contrast, the proposed algorithm effectively suppresses clutter across the range, resulting in distinct peaks at the target ranges, enabling clear target sensing.

The RMSE results of the target's parameter estimation over the speed of a moving ISAC transceiver are shown in Fig. 5, comparing the algorithm of H.Luo et al. [15] and the proposed ISAC-STAP. Here, Fig. 5a and Fig. 5b are the RMSEs of angle estimation and radial velocity estimation, respectively. Fig. 5a shows that the angle estimation RMSE of both H. Luo et al. [15] and ISAC-STAP are low when the ISAC transceiver's speed is zero. However, the angle estimation performance of H. Luo et al. [15] significantly decreases as the transceiver

speed increases. Since H. Luo et al. [15] suppressed the signal with zero velocity, the target's angle estimation performance is degraded due to the remaining clutter. In contrast, the proposed algorithm maintains a stable angle estimation RMSE regardless of the transceiver's speed since it successfully suppresses the clutter. Moreover, the RMSE result of radial velocity shows a similar tendency as shown in Fig. 5b due to the aforementioned reason. The simulation results of Fig. 5a and Fig. 5b indicate that the proposed algorithm is the best option for the mobile ISAC system.

V. Conclusion

In this paper, we present an ISAC-STAP algorithm for a moving ISAC transceiver. The proposed algorithm first pre-processes the echo signal by converting the subcarrier domain to the range domain to obtain target-free clutter information. After pre-processing, the spatio-temporal adaptive filter is applied to suppress clutter, improving the target sensing performance. Simulation results show that the proposed algorithm is superior to the benchmark algorithm in mobile ISAC systems. Further extension is developing the efficient target sensing algorithm to account for more complex environments, such as dynamic interference between vehicles and non-line-of-sight (NLOS) conditions in mobile ISAC systems.

References

[1] F. Liu, Y. Cui, C. Masouros, J. Xu, T. X. Han, Y. C. Eldar, and S. Buzzi, "Integrated sensing and communications: Toward dual-functional wireless networks for 6G and beyond," *IEEE J. Sel. Areas Commun.*, vol. 40, no. 6, pp. 1728–1767, 2022.

[2] Z. Wei, H. Qu, Y. Wang, X. Yuan, H. Wu, Y. Du, K. Han, N. Zhang, and Z. Feng, "Integrated sensing and communication signals toward 5G-A and 6G: A survey," *IEEE Internet Things J.*, vol. 10, no. 13, pp. 11 068–11 092, 2023.

[3] J. A. Zhang, M. L. Rahman, K. Wu, X. Huang, Y. J. Guo, S. Chen, and J. Yuan, "Enabling joint communication and radar sensing in mobile networks—A survey," *IEEE Commun. Surv. Tutor.*, vol. 24, no. 1, pp. 306–345, 2022.

[4] F. Liu, C. Masouros, A. P. Petropulu, H. Griffiths, and L. Hanzo, "Joint radar and communication design: Applications, state-of-the-art, and the road ahead," *IEEE Trans. Commun.*, vol. 68, no. 6, pp. 3834–3862, 2020.

[5] "Hexa-X-II project," Accessed on: Jun. 27, 2024. [Online]. Available: https://hexa-x-ii.eu/.

[6] "Draft New Recommendation ITU-R M. [IMT. FRAMEWORK 2030 BEYOND]," ITU-R WP5D. 2023.

[7] G. Kwon, Z. Liu, A. Conti, H. Park, and M. Z. Win, "Integrated localization and communication for efficient millimeter wave networks," *IEEE J. Sel. Areas Commun.*, vol. 41, no. 12, pp. 3925–3941, 2023.

[8] F. Gao, L. Xu, and S. Ma, "Integrated sensing and communications with joint beam-squint and beam-split for mmWave/THz massive MIMO," *IEEE Trans. Commun.*, vol. 71, no. 5, pp. 2963–2976, 2023.

[9] J. A. Zhang, F. Liu, C. Masouros, R. W. Heath, Z. Feng, L. Zheng, and A. Petropulu, "An overview of signal processing techniques for joint communication and radar sensing," *IEEE J. Sel. Top. Signal Process.*, vol. 15, no. 6, pp. 1295–1315, 2021.

[10] S. Lu, F. Liu, Y. Li, K. Zhang, H. Huang, J. Zou, X. Li, Y. Dong, F. Dong, J. Zhu, Y. Xiong, W. Yuan, Y. Cui, and L. Hanzo, "Integrated sensing and communications: Recent advances and ten open challenges," *IEEE Internet Things J.*, vol. 11, no. 11, pp. 19 094–19 120, 2024.

[11] Y. Niu, Z. Wei, L. Wang, H. Wu, and Z. Feng, "Interference management for integrated sensing and communication systems: A survey," *arXiv preprint arXiv:2403.16189*, 2024.

[12] X. Cheng, D. Duan, S. Gao, and L. Yang, "Integrated sensing and communications (ISAC) for vehicular communication networks (VCN)," *IEEE Internet Things J.*, vol. 9, no. 23, pp. 23 441–23 451, 2022.

[13] C. Liao, F. Wang, and V. K. Lau, "Optimized design for IRS-assisted integrated sensing and communication systems in clutter environments," *IEEE Trans. Commun.*, vol. 71, no. 8, pp. 4721–4734, 2023.

[14] R. Liu, M. Li, Q. Liu, and A. L. Swindlehurst, "Joint waveform and filter designs for STAP-SLP-Based MIMO-DFRC systems," *IEEE J. Sel. Areas Commun.*, vol. 40, no. 6, pp. 1918–1931, 2022.

[15] H. Luo, Y. Wang, D. Luo, J. Zhao, H. Wu, S. Ma, and F. Gao, "Integrated sensing and communications in clutter environment," *IEEE Trans. Wireless Commun.*, pp. 1–1, 2024.

[16] Y. Geng, "A search space-based clutter mitigation algorithm for ISAC systems," in *Proc. IEEE Int. Conf. Commun. Workshops*, 2024, pp. 2065–2070.

[17] H. Chen, H. Sarieddeen, T. Ballal, H. Wymeersch, M.-S. Alouini, and T. Y. Al-Naffouri, "A tutorial on Terahertz-band localization for 6G communication systems," *IEEE Commun. Surv. Tutor.*, vol. 24, no. 3, pp. 1780–1815, 2022.

[18] M. H. C. Garcia, A. Molina-Galan, M. Boban, J. Gozalvez, B. Coll-Perales, T. Şahin, and A. Kousaridas, "A tutorial on 5G NR V2X communications," *IEEE Commun. Surv. Tutor.*, vol. 23, no. 3, pp. 1972–2026, 2021.

[19] A. Goldsmith, *Wireless communications*. Cambridge university press, 2005.

[20] W. Melvin, "A STAP overview," *IEEE Aerosp. Electron. Syst. Mag.*, vol. 19, no. 1, pp. 19–35, 2004.

[21] I. Reed, J. Mallett, and L. Brennan, "Rapid convergence rate in adaptive arrays," *IEEE Trans. Aerosp. Electron. Syst.*, vol. AES-10, no. 6, pp. 853–863, Nov. 1974.